

## Deconfinement and Chiral Symmetry Restoration in an $SU(3)$ Gauge Theory with Adjoint Fermions

Frithjof Karsch and Martin Lütgemeier

Fakultät für Physik, Universität Bielefeld, D-33615 Bielefeld, Germany

### ABSTRACT

We analyze the finite temperature phase diagram of  $QCD$  with fermions in the adjoint representation. The simulations performed with four dynamical Majorana fermions show that the deconfinement and chiral phase transitions occur at two distinct temperatures. While the deconfinement transition is first order at  $T_d$  we find evidence for a continuous chiral transition at a higher temperature  $T_c \simeq 8 T_d$ . We observe a rapid change of bulk thermodynamic observables at  $T_d$  which reflects the increase in the number of degrees of freedom. However, these show little variation at  $T_c$ , where the fermion condensate vanishes. We also analyze the potential between static fundamental and adjoint charges in all three phases and extract the corresponding screening masses above  $T_d$ .

# 1 Introduction

The interplay between confinement and chiral symmetry restoration is one of the most puzzling problems in finite temperature  $QCD$ . Both phenomena seem to refer to different non perturbative mechanisms, where a priori unrelated length scales are involved. But speculations, that  $QCD$  would therefore undergo two distinct phase transitions [1] - deconfinement of quarks and gluons at  $T_d$  followed by the restoration of chiral symmetry at some higher temperature  $T_c$  - could not be confirmed by lattice calculations. The two effects seem to be tightly coupled in  $QCD$ . At a unique critical temperature the chiral condensate vanishes and the asymptotic value of the heavy-quark potential drops rapidly indicating deconfinement.

Thermodynamic quantities calculated in the vicinity of the  $QCD$  phase transition temperature exhibit the deconfining as well as chiral symmetry restoring aspects of this transition. Observables like the energy or entropy density show a sudden rise at  $T_c$  which reflects the liberation of many new partonic degrees of freedom due to deconfinement. In this respect the transition is very similar to that in the pure gauge sector where quarks are absent and chiral symmetry thus does not play a role. In  $QCD$  with  $n_f$  light quark flavours, however, also the chiral condensate drops rapidly and vanishes at  $T_c$  for vanishing quark masses. In fact, it generally is believed that details of the  $QCD$  phase transition, e.g. the order of the transition, is controlled by chiral symmetry. At least qualitatively this has been confirmed by numerical calculations. While the transition is first order for  $QCD$  with three or more light flavours it does seem to be continuous for two flavours as expected from general universality arguments [2], although at present the analysis of critical exponents for two flavour ( $n_f = 2$ )  $QCD$  is not entirely in agreement with expectations based on the universality class of 3-dimensional  $O(4)$  spin models [4, 5]. Also characteristic chiral singularities, which are expected to show up in the quark mass dependence of the chiral susceptibility for  $T \lesssim T_c$  [6] have so far not been observed.

In how far are the chiral properties of the transition dependent on the confinement-deconfinement transition and in how far is chiral symmetry restoration reflected in the behaviour of bulk thermodynamic observables? In order to get further insight into these questions one may analyze  $QCD$  related models in which both transitions fall apart. The  $SU(N)$  gauge theories with fermions in the adjoint representation ( $aQCD$ ) offer this possibility. Early investigations of  $SU(2)$  with two<sup>a</sup> adjoint fermions [7, 8] indeed suggest that the two phase transitions are well separated with  $T_d < T_c$ . This may not be too surprising as  $aQCD$  possesses two distinct global symmetries. Unlike fermions in the fundamental representation the adjoint fermions do not break the global  $Z(N)$  center symmetry of the  $SU(N)$  gauge group. The model

---

<sup>a</sup>In the following we will adopt the  $QCD$  convention when counting the number of fermion flavours, i.e. we count the number of Dirac fermion species in the adjoint representation rather than Majorana fermions.

thus has the  $Z(N)$  center symmetry and a  $SU(2n_f)$  chiral symmetry [9, 10]. At low temperatures the latter is broken down to  $SO(2n_f)$  while the former is expected to become broken at high temperature. Related to these symmetries and their breaking or restoration are two order parameters, the Polyakov loop expectation value and the expectation value of the fermion condensate, which can characterize the different phases of the theory<sup>b</sup>.

In this paper we concentrate on an analysis of the thermodynamics of  $aQCD$ . We determine the critical temperatures, analyze the order of the transitions and give an estimate of the latent heat at the deconfinement transition. Particular emphasis is put on the investigation of the thermodynamics in the intermediate phase, *i.e.* for  $T_d < T < T_c$ , where we analyze the temperature and fermion mass dependence of the fermion condensate, its susceptibility as well as potentials for static fermions in the fundamental and adjoint representations. Before discussing the thermodynamics of  $aQCD$  in section 3 we will introduce the model and give a description of numerical aspects of our calculations in section 2. Section 4 contains our conclusions.

## 2 $SU(3)$ gauge theory with fermions in the adjoint representation: aQCD

In this section we want to introduce the basic properties of the lattice formulation of the  $SU(3)$  gauge theory with fermions in the adjoint representation. We will use for our investigations the standard Wilson one-plaquette gauge action. In the fermion sector we use the staggered fermion formulation. The only modification compared to  $QCD$  calculations is that the fermions are in the adjoint (8-dimensional) representation of the  $SU(3)$  group. As they carry now eight colour degrees of freedom we also need an 8-dimensional representation for the gluon fields in the discretization of the fermionic action,

$$S = \beta S_G + \sum_{x,y} \bar{\psi}_x M(U^{(8)})_{x,y} \psi_y \quad , \quad (1)$$

where  $M(U^{(8)})$  denotes the standard staggered fermion matrix with the 3-dimensional gauge field matrices  $U^{(3)}$  replaced by the 8-dimensional representation  $U^{(8)}$ ,  $\beta = 6/g^2$  is related to the inverse coupling of the gauge fields and  $S_G$  denotes the gluonic part

---

<sup>b</sup>We note that the model we are discussing here is closely related to supersymmetric gauge theories. For a recent attempt to simulate supersymmetric Yang Mills theories on the lattice see [11]. The possibility of the breaking of the  $Z(N)$  center symmetry in finite temperature supersymmetric models has recently also been discussed in Ref. [12].

of the action,

$$S_G = \sum_{\square} \left\{ 1 - \frac{1}{3} \text{ReTr} U_{\square}^{(3)} \right\} . \quad (2)$$

We note that the 8-dimensional representation may be represented in terms of the 3-dimensional one as

$$U_{ab}^{(8)} = \frac{1}{2} \text{tr} [\lambda_a U^{(3)} \lambda_b U^{(3)\dagger}] , \quad (3)$$

with  $\lambda_a$  being the Gell-Mann matrices and  $\text{tr}$  the 3-trace. This also shows explicitly that the action for adjoint fermions does not break the  $Z(3)$  center symmetry. In the fermionic part of the action the matrices  $U^{(3)}$  appear only in complex conjugate pairs  $U^{(3)}$ ,  $U^{(3)\dagger}$ . The two center elements appearing in a  $Z(3)$  transformation therefore cancel each other. Like in the  $SU(3)$  gauge theory the Polyakov loop,

$$L_3 \equiv \lim_{N_{\sigma} \rightarrow \infty} \left\langle \frac{1}{N_{\sigma}^3} \left| \sum_{\vec{x}} L_3(\vec{x}) \right| \right\rangle = \lim_{N_{\sigma} \rightarrow \infty} \left\langle \frac{1}{3N_{\sigma}^3} \left| \sum_{\vec{x}} \text{Tr} \prod_{x_0=1}^{N_{\tau}} U^{(3)}(x_0, \vec{x}) \right| \right\rangle , \quad (4)$$

thus still is an order parameter of the theory for the spontaneous breaking of the center symmetry. As its value is related to the asymptotic behaviour of the Polyakov loop correlation function,

$$\exp(-V_3(\vec{x}, T)/T) \equiv \langle L_3(\vec{0}) L_3^{\dagger}(\vec{x}) \rangle \xrightarrow{|\vec{x}| \rightarrow \infty} L_3^2 , \quad (5)$$

which defines the potential between static fundamental charges, it is obvious that the thermal medium generated by  $aQCD$  will be confining for fundamental charges at low temperatures as long as the  $Z(3)$  center symmetry is not spontaneously broken. In contrast to this the expectation value of the adjoint Polyakov loop<sup>c</sup>,

$$L_8 \equiv \lim_{N_{\sigma} \rightarrow \infty} \left\langle \frac{1}{N_{\sigma}^3} \sum_{\vec{x}} L_8(\vec{x}) \right\rangle = \lim_{N_{\sigma} \rightarrow \infty} \left\langle \frac{1}{8N_{\sigma}^3} \sum_{\vec{x}} \text{Tr} \prod_{x_0=1}^{N_{\tau}} U^{(8)}(x_0, \vec{x}) \right\rangle , \quad (6)$$

is non-zero for all values of  $\beta$ . Adjoint charges are thus screened and the corresponding potential reaches a constant value at large distances<sup>d</sup>,

$$\exp(-V_8(\vec{x}, T)/T) \equiv \langle L_8(\vec{0}) L_8(\vec{x}) \rangle \xrightarrow{|\vec{x}| \rightarrow \infty} L_8^2 . \quad (7)$$

<sup>c</sup>To evaluate adjoint traces we may use the relation  $\text{Tr} U^{(8)} = |\text{Tr} U^{(3)}|^2 - 1$ , which can easily be derived from equation 3.

<sup>d</sup>Note that this screening is not only related to the fact that adjoint charges appear now as dynamical degrees of freedom in  $aQCD$ . Even in the quenched case, *i.e.* the pure  $SU(3)$  gauge theory, adjoint charges are screened at low temperatures. String breaking has been analyzed in this limit [15].

We note that the matrices  $U^{(8)}$  are real and so is the entire fermion matrix  $M$  and its determinant. As a consequence of this pseudo fermion fields  $\Phi$ , which are generally used to represent the fermion determinant as a Gaussian integral over bosonic fields, can be chosen real. This reduces the number of fermion doublers by a factor of 2, *i.e.* we can set up an exact fermion algorithm for two adjoint fermion flavours (see footnote a).

The pseudo fermion action, used in our simulations thus reads

$$S = \beta \sum_{\square} \left\{ 1 - \frac{1}{3} \text{ReTr} U_{\square}^{(3)} \right\} + \Phi^t \left\{ M(U^{(8)})^t M(U^{(8)}) \right\}^{-1} \Phi \quad . \quad (8)$$

For our calculations we use the hybrid Monte Carlo algorithm. We note that the entire molecular dynamics evolution of the system can be expressed in terms of the 3-dimensional matrices  $U^{(3)}$  and the fermion fields. An explicit representation of the matrices  $U^{(8)}$  is only needed in the conjugate gradient routine used for the inversion of the fermion matrix. Technically the largest problem this prescription causes is the evaluation of the time derivative of  $M^t M$ , which is needed in the molecular dynamics steps. As the fermion matrix now is quadratic in  $U^{(3)}$  time derivatives generate also twice as many terms in the Hamiltonian evolution equations as in ordinary *QCD* simulations.

Our simulations were performed on lattices of size  $N_{\sigma}^3 \times N_{\tau}$  with  $N_{\tau} = 4$  and  $N_{\sigma} = 8$  and 16. On the smaller lattice we performed simulations for 15  $\beta$ -values in the interval  $[5.2; 6.5]$  each for the bare masses  $m = 0.02, 0.04, 0.08, 0.10$ . In some cases additional runs were performed at a smaller fermion mass,  $m = 0.01$ , as well as at intermediate masses,  $m = 0.03$  and  $m = 0.05$ . On the larger lattice calculations were performed with the fermion mass  $m = 0.02$  for 8  $\beta$ -values between 5.25 and 6.5. At some selected values of the gauge coupling,  $\beta = 5.25, 5.4, 6.2, 6.5$ , which were chosen in the three different phases of thermal *aQCD*, we also calculated the fundamental and adjoint Polyakov loop correlation functions and extracted the corresponding potentials from them.

We used the hybrid- $\Phi$  algorithm [3] with the standard gluon and staggered fermion action only modified for the adjoint representation, and the conjugate gradient method for the inversion of the fermion matrix. The residuum was  $10^{-8}$  inside the molecular dynamic steps and  $10^{-13}$  elsewhere. The length of a trajectory has been fixed to  $\Delta t = 0.25$ . The number of subdivisions of a trajectory has been chosen such that we reached an acceptance rate of 60 – 80% which could drop to 50% in the vicinity of  $\beta_d$ . It turned out that the number of subdivisions needed mainly depends on the fermion mass and shows little dependence on  $\beta$ . More details on our simulation parameters are given in Table 1.

mass	#mol.dyn. steps	#traj. for therm.	#traj. for measurement
$8^3 \times 4$ lattice			
0.01	64	500	1000 - 3000
0.02	40	500	1500 - 6500
0.03	32	500	1500
0.04	28	500	2800 - 7500
0.05	25	500	2500 - 6500
0.08	21	500 - 1000	1500 - 7000
0.10	20	500 - 1000	400 - 14000
$16^3 \times 4$ lattice			
0.02	50-75	100 - 1000	500 - 2300

Table 1: Parameters used in the hybrid Monte Carlo calculations on different lattice sizes and for different values of the fermion mass.

Plaquette and Polyakov loop expectation values have been calculated on every configuration, the fermion condensate only on every 5th for the small lattice and every second configuration for the larger lattice. On these configurations we also calculated the disconnected part of the fermionic susceptibility [4],

$$\chi_m = \frac{1}{N_\sigma^3 N_\tau} \left( \langle (\text{Tr} M^{-1})^2 \rangle - \langle \text{Tr} M^{-1} \rangle^2 \right) \quad (9)$$

for which we used a noisy estimator [13] with 25 random source vectors.

Correlation functions of Polyakov loops for fundamental and adjoint static fermions have been calculated in order to extract the potential for both types of fermions. The correlators were measured every second iteration at distances  $R = \sqrt{x_1^2 + x_2^2 + x_3^2}$ ,  $x_i = 0, 1, 2, 3, 4$  and also at on-axis distances 5, 6, 7 and 8. After averaging over correlations at equal distance we obtained the potentials at 33 points for  $1.0 \leq R \leq 8.0$ .

### 3 Thermodynamics of $aQCD$

As discussed in the previous section the Polyakov loop,  $L_3$ , is an order parameter for the spontaneous breaking of the  $Z(3)$  center symmetry of  $aQCD$  and easily is

related to the confining/deconfining properties of the static potential for fundamental charges (Eq. 5). Less obvious is that this also reflects the deconfinement of the dynamical degrees of freedom of  $aQCD$ , *i.e.* the adjoint fermions. In order to analyze this question we have calculated various observables reflecting thermodynamic properties of the hot medium which we will discuss in the following. We will start with a discussion of signals for the deconfinement and chiral transitions and then discuss thermodynamic observables related to the equation of state of  $aQCD$ .

### 3.1 Deconfinement phase transition

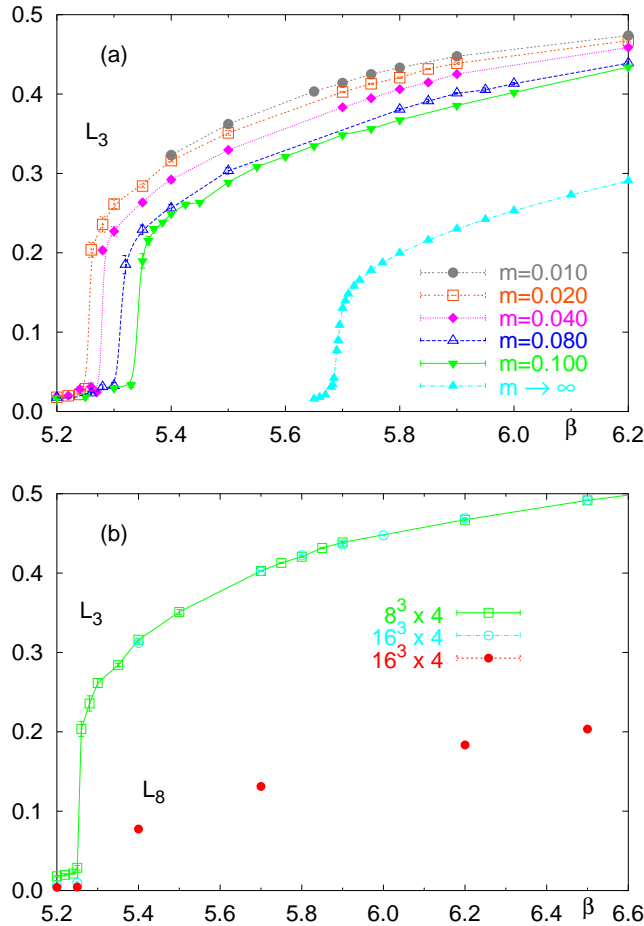


Figure 1: Expectation value of the absolute value of the Polyakov loop for the fundamental representation,  $L_3$ , versus coupling,  $\beta = 6/g^2$ , calculated on lattices of size  $8^3 \times 4$  (a). Shown are results from simulations with different fermion masses and a result from simulations in the pure gauge sector ( $m \rightarrow \infty$ ). Figure 1b gives a comparison of results from two different lattice sizes for  $m = 0.02$  and in addition also shows the adjoint Polyakov loop  $L_8$ .

In Figure 1 we show results for the Polyakov loop expectation values in the funda-

m	0.10	0.08	0.04	0.02	0.0
$\beta_d(m)$	5.342 (2)	5.312 (2)	5.279 (2)	5.256 (2)	5.236 (3)

Table 2: Critical couplings for the deconfinement transition estimated on lattices of size  $8^3 \times 4$  and for different fermion masses. The last column shows the result of a linear extrapolation to the zero fermion mass limit.

mental and adjoint representation. The Polyakov loop for fermions in the fundamental representation shows a clear jump around  $\beta = 5.3$ . The size of the discontinuity does not indicate a significant dependence on the fermion mass in the range covered by our simulations. It is, however, much larger than in the quenched ( $m \rightarrow \infty$ ) limit, which also is shown in Figure 1. This is in accordance with the stronger screening observed for the static heavy fermion potential (see discussion below). We also note that the adjoint Polyakov loop changes from small but non-zero values to large non-zero values above  $T_d$ , which also signals a sudden change in the potential for static adjoint charges.

Using the reweighting method of Ferrenberg-Swendsen [14] we have located the peak of the Polyakov loop susceptibilities,

$$\chi_L = N_\sigma^3 \left( \left\langle \left| \frac{1}{N_\sigma^3} \sum_{\vec{x}} L_3(\vec{x}) \right|^2 \right\rangle - L_3^2 \right) \quad , \quad (10)$$

at fermion masses  $m = 0.02, 0.04, 0.08, 0.10$ . This gives estimates for the critical couplings<sup>e</sup> which were used for an extrapolation to the  $m = 0$  limit with a general ansatz,  $\beta_d(m) = \beta_d(0) + c \cdot m^\alpha$ . It turns out that the exponent  $\alpha$  is unity within statistical errors. Finally, we thus performed an extrapolation using  $\alpha = 1$ . This yields  $\beta_d(0) = 5.236(3)$ . We will use this value of the critical coupling in the next subsection to determine the relation between the critical temperatures for deconfinement and chiral symmetry restoration.

In Figure 2 we show the potentials for static charges in the fundamental and adjoint representations calculated at two temperatures below and above  $T_d$  on lattices of size  $16^3 \times 4$ . They clearly show the sudden change from a strictly confining (fundamental charges) or confinement + string breaking (adjoint charges) potential at low temperatures to a screened potential above  $T_d$ . We note that for  $T \lesssim T_d$  the breaking of the adjoint string does set in quite early, *i.e.* already at distances  $R \sim 0.6/T$ . For smaller distances the linear rise of the fundamental and adjoint potentials is compatible, *i.e.* we do not see indications for a Casimir scaling as it has been observed in pure  $SU(3)$  gauge theories at zero temperature [15]. Below  $T_d$  the potentials shown

---

<sup>e</sup>We did not aim at a more precise determination of the critical points and thus did not analyze further their volume dependence.



	$\alpha$	$\mu/T$
fundamental	0.11 (4)	6.4 (6)
adjoint	0.28 (9)	5.6 (6)

Table 3: Screening masses in units of the temperature,  $\mu/T$ , and the Coulomb coefficient of the static potentials for fundamental and adjoint fermions at  $\beta = 5.4$  calculated on  $16^3 \times 4$  lattice with adjoint fermions of mass  $m = 0.02$ .

in Figure 2 have, in fact, been calculated at a temperature quite close to  $T_d$ . This can be estimated by using the 2-loop  $\beta$ -function for  $aQCD$ ,

$$a\Lambda_L = R(\beta) \approx \left(\frac{6b_0}{\beta}\right)^{-\frac{b_1}{2b_0^2}} \exp\left(-\frac{\beta}{12b_0}\right) \quad , \quad (11)$$

with coefficients  $b_0, b_1$  appropriate for  $SU(3)$  with two flavours in the adjoint representation, *i.e.*  $b_0 = 3/(16\pi^2)$  and  $b_1 = 115/(384\pi^4)$ . From this we conclude that our calculation at  $\beta = 5.25$  for  $m = 0.02$  corresponds to a temperature  $T \simeq 0.97T_d$ . At this temperature we still find quite a large value of the string tension. A fit to the potential for fundamental charges yields  $\sqrt{\sigma}(T)/T = 1.98$  (4), which should be compared to a calculation in the pure gauge sector close to the critical temperature [16] which gave  $\left(\sqrt{\sigma}(T)/T\right)_{SU(3)} = 0.93$  (3). This shows that the deconfinement transition in  $aQCD$  is strongly first order with a large discontinuity in the string tension. We will find further support for this conclusion from the analysis of the latent heat at  $T_d$  which will be discussed in section 3.3.

Above  $T_d$  the static potentials are strongly screened. We have tried to extract a screening mass by fitting the potentials with an ansatz for a Debye screened Coulomb potential,

$$\frac{V(R)}{T} = -\frac{\alpha}{RT} e^{-\mu R}. \quad (12)$$

The results from such a fit are given in Table 3. Although the statistical errors are of the order of 10% one sees that the screening masses for fundamental and adjoint charges are in agreement with each other, while the coupling strength is different. We note that similar studies in the pure gauge sector gave screening masses which are about half as large,  $\mu/T \simeq 2-3$ . This gives support to a picture where screening of the fundamental and adjoint potentials in  $aQCD$  results from the exchange of gluons with an effective thermal mass that is larger than in  $QCD$  because it now receives contributions from internal gluon and adjoint fermion loops.

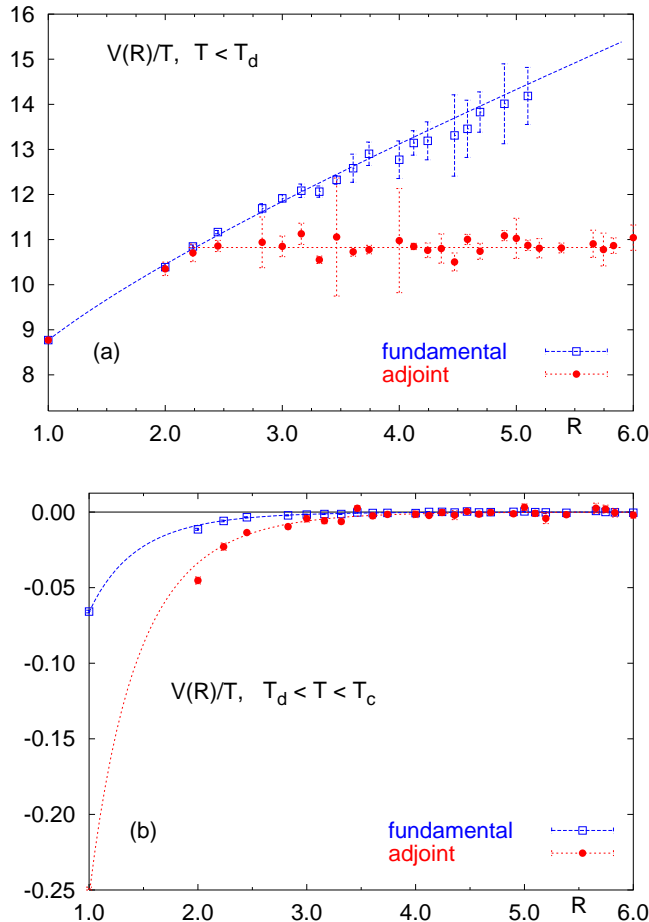


Figure 2: Static potentials for fundamental and adjoint charges calculated below (a) and above (b)  $T_d$  on lattices of size  $16^3 \times 4$  at  $\beta = 5.25$  and  $5.4$ , respectively. Calculations have been performed with fermion mass  $m = 0.02$ . The lines show fits as discussed in the text. For  $\beta = 5.25$  the potentials have been normalized at  $R = 1$ . Also note the different scales in (a) and (b).

### 3.2 Chiral phase transition

Let us now turn to a discussion of the fermion condensate (Figure 3). It clearly feels the deconfinement transition and is discontinuous at  $\beta_d$ . For  $\beta > \beta_d$  it, however, remains nonzero and large. For non-zero fermion masses this is, of course, expected. In order to decide, if the chiral symmetry indeed remains broken above  $T_d$ , one has to extrapolate to the chiral limit,  $m = 0$ . However, before doing so we want to discuss the fermion mass dependence of the fermionic susceptibility, Eq. 9. At the critical temperature of a second order chiral phase transition the susceptibility is expected to diverge like  $m^{-(1-1/\delta)}$ , where universality relates the critical exponent  $\delta$  to that of the  $O(6)$  model in three dimensions ( $\delta \simeq 5$ ). For finite fermion masses this singular behaviour shows up as a peak in the susceptibility at some pseudo-critical

coupling  $\beta_c(m)$  at which the peak height shows the same fermion mass dependence,  $\chi_{m,\max} \sim m^{-(1-1/\delta)}$ . At least qualitatively this behaviour, *i.e.* pronounced peaks of the susceptibility at some pseudo-critical coupling, has been observed in *QCD* with light quarks in the fundamental representation. The close relation to the  $\sigma$ -models in three dimensions established by universality arguments also suggests that the fermionic susceptibility diverges below  $T_c$  in the zero fermion mass limit like  $m^{-1/2}$  [6]. For small fermion masses the divergence at  $T_c$  will, however, be stronger ( $1 - 1/\delta \simeq 0.8$ ) and the chiral transition should still be signaled by a peak in the susceptibility. So far, the presence of the divergence of  $\chi_m$  below  $T_c$  could not be verified in *QCD*. To some extent this may be due to the strong shift of the pseudo-critical couplings with quark mass,  $\beta_c(m)$ , which makes an analysis of  $\chi_m$  for constant temperatures below but close to  $T_c$  difficult in *QCD*. As will become clear below these characteristic singularities induced by the fluctuations of the Goldstone modes are, however, clearly visible in *aQCD* just because of the clear separation of the deconfinement and chiral phase transitions.

In Figure 3 we show the fermionic susceptibilities of *aQCD* for several values of the fermion mass. First of all it is evident that the singularity related to the breaking of the  $Z(3)$  symmetry is also clearly visible in  $\chi_m$ . For temperatures above  $T_d$  the susceptibility does, however, show quite an unusual behaviour not easily visible in *QCD* simulations with fermions in the fundamental representation. Above  $T_d$  there exists a long, strongly mass dependent plateau at the end of which a second peak starts developing for the smallest fermion masses used in our simulation, *i.e.* for  $m = 0.02$  and  $m = 0.01$ . As can be seen in Figure 4 this plateau indeed rises like  $1/\sqrt{m}$  as expected from the analysis of Goldstone modes in the three dimensional  $\sigma$ -models [6]. Only close to  $T_c$  the susceptibilities start rising faster and thus reflect the more singular behaviour at  $T_c$ . In this region one thus would expect that the appropriate form to extrapolate the fermion condensate is given by the ansatz,

$$\langle \bar{\psi}\psi \rangle = a_0 + a_1 m^{1/2} \quad . \quad (13)$$

This is indeed supported by the numerical results shown in Figure 3. For larger fermion masses, of course higher order corrections become relevant. In the intermediate regime  $5.4 < \beta < 5.8$  we therefore have analyzed the data for the fermion condensate using the general ansatz

$$\langle \bar{\psi}\psi \rangle(\beta, m) = a_0 + \bar{a}_1 m^{1/2} + a_1 m + a_2 m^2 + a_3 m^3 \quad . \quad (14)$$

For couplings  $\beta > 5.8$  we have used this ansatz with  $\bar{a}_1 \equiv 0$ . The resulting extrapolation for the fermion condensate is also shown in Figure 3. This clearly demonstrates that the fermion condensate remains non-zero above  $T_d$  and only vanishes at a larger temperature  $T_c$  corresponding to a critical coupling  $\beta_c \simeq 5.8$ .

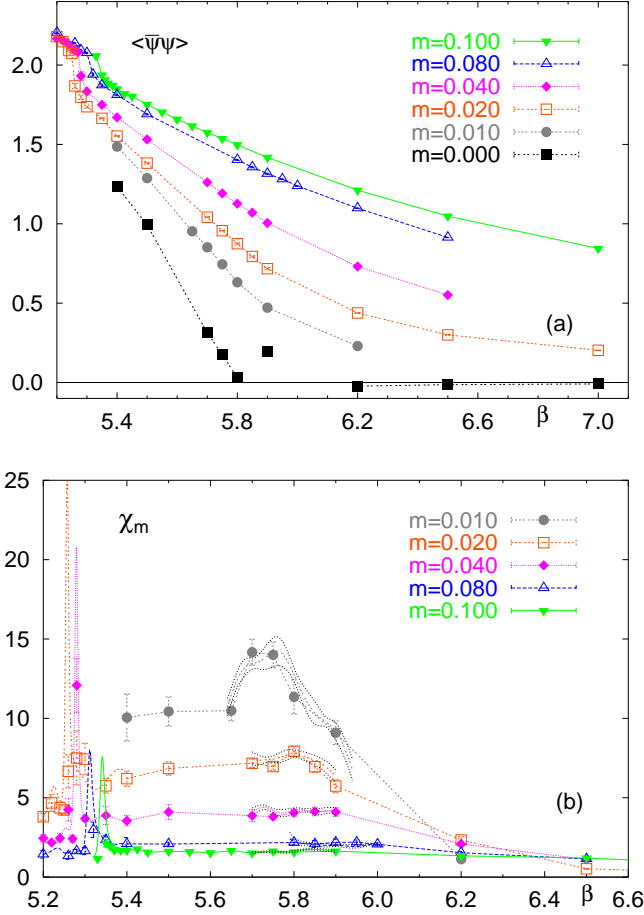


Figure 3: Fermion condensate (a) and fermionic susceptibility (b) calculated on lattices of size  $8^3 \times 4$  for several values of the fermion mass. In Figure 3a we also show the result of an extrapolation to  $m = 0$  (see text). Also shown in Figure 3b are interpolating curves with the corresponding error band obtained with the help of the Ferrenberg-Swendsen reweighting method.

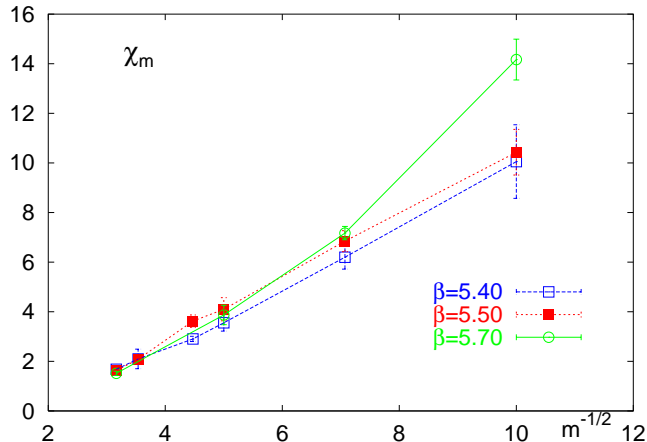


Figure 4: Chiral susceptibility versus  $1/\sqrt{m}$  at three values of the gauge coupling in the intermediate phase, *i.e.* for  $T_d < T < T_c$ .

mass	0.02	0.01
$\beta_c$	5.80 (3)	5.77 (3)

Table 4: Pseudo-critical couplings for the chiral transition determined from the location of peaks in the fermionic susceptibilities on lattices of size  $8^3 \times 4$ .

The critical coupling,  $\beta_c$ , may also be estimated from the location of the peaks in  $\chi_m$ , which become visible for small fermion masses. The corresponding pseudo-critical couplings extracted from a Ferrenberg-Swendsen interpolation are given in Table 4. This is in accordance with our extrapolation of the fermion condensate. We thus obtain as an estimate for the critical couplings of the chiral and deconfinement transitions in the zero mass limit

$$\begin{aligned}
 \beta_d &= 5.236 \pm 0.003 \quad , \\
 \beta_c &= 5.79 \pm 0.05 \quad .
 \end{aligned}
 \tag{15}$$

The difference between these critical couplings may be used to estimate the ratio of the critical temperatures for deconfinement and chiral symmetry restoration in *aQCD*. To do so we use the 2-loop  $\beta$ -function, Eq. 11. This yields<sup>f</sup>

$$T_c/T_d \approx 7.7 \pm 2.1 \quad .
 \tag{16}$$

<sup>f</sup>Using only the one-loop formula one obtains  $T_c/T_d = 11.9 \pm 2.8$ . Note that this is much smaller than the estimate given in Ref. [7] for the case of  $SU(2)$ ,  $T_c/T_d = 175 \pm 50$ .

We stress that so far no detailed investigation of the approach of lattice regularized  $aQCD$  to the continuum limit exists. If violations of asymptotic scaling turn out to be similar in magnitude to those found in the pure  $SU(3)$  gauge theory this ratio may well be underestimated by a factor of two.

### 3.3 Latent heat and pressure close to $T_d$

In the previous subsections we have collected evidence for two separate phase transitions in  $aQCD$ . Let us now address in somewhat more detail the question how these transitions influence the equation of state of  $aQCD$ . The basic quantity we want to discuss here is the pressure as function of temperature. In numerical calculations one has direct access to the free energy density in units of  $T^4$ , *i.e.*  $f/T^4$  [17, 18]. In the thermodynamic limit this is directly related to the pressure,  $p/T^4 = -f/T^4$ . The free energy density is obtained from an integration over the difference of gluonic actions,  $\langle S_G \rangle$ , calculated at zero and non-zero temperature. The former only serves to normalize the pressure correctly, all significant changes in the pressure as function of temperature are, however, visible already in the expectation value of the gluonic action. In particular, the first order deconfinement phase transition also leads to a discontinuity  $\langle \Delta S_G \rangle$ , which directly is related to the latent heat at  $T_d$ ,

$$\frac{\Delta \epsilon}{T^4} = \frac{\Delta(\epsilon - 3p)}{T^4} = -a \frac{d\beta}{da} \cdot \left( \frac{N_\tau}{N_\sigma} \right)^3 \cdot \langle \Delta S_G \rangle . \quad (17)$$

Here  $\langle \Delta S_G \rangle = \langle S_G \rangle_- - \langle S_G \rangle_+$  denotes the difference of action expectation values calculated at  $T_d$  in the confined ( $-$ ) and deconfined ( $+$ ) phase, respectively.  $S_G$  is given by Eq. 2 and  $-ad\beta/da$  is the  $\beta$ -function of  $aQCD$ . The latter should be determined non-perturbatively at the critical coupling  $\beta_d$ . As a first estimate for the latent heat it is, however, sufficient to use the asymptotic 2-loop relation, Eq. 11, between the gauge coupling  $\beta$  and the lattice spacing  $a$ . A similar approach has also been used to estimate the latent heat at the deconfinement transition in a  $SU(3)$  gauge theory [19] and we thus can compare our results with this calculation.

In Figure 5 we show the plaquette expectation values which are related to the expectation value of the gluonic part of the action through

$$\langle P \rangle = 1 - \frac{1}{6N_\tau N_\sigma^3} \langle S_G \rangle . \quad (18)$$

Even on the rather small lattice used by us ( $8^3 \times 4$ ) the rapid change at  $T_d$  is clearly visible. A comparison with results obtained in the pure gauge theory ( $m \rightarrow \infty$ ) on larger lattices shows, in fact, that the discontinuity in  $\langle S_G \rangle$  is much larger in the

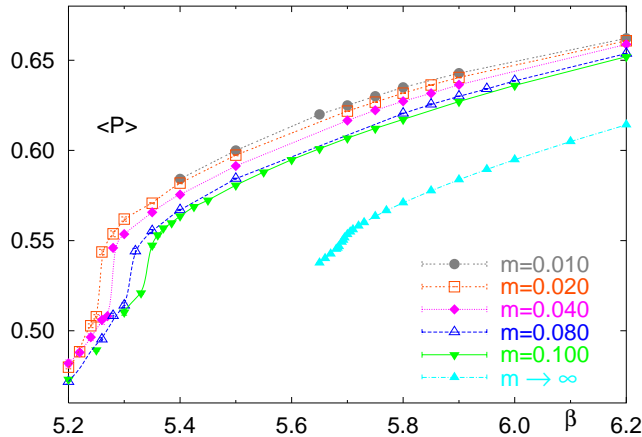


Figure 5: Normalized expectation values of the gluon action defined by Eq. 18 (plaquette expectation value) for different fermion masses on lattices of size  $8^3 \times 4$ . Also shown is the corresponding result obtained in the pure gauge sector ( $m \rightarrow \infty$ ) on a  $16^3 \times 4$  lattice.

light fermion mass limit of  $aQCD$ . This also is evident from the probability distribution of plaquette values, which shows in all cases a clear double peak structure. Again we have used the Ferrenberg-Swendsen reweighting to construct the plaquette distributions at  $\beta_c(m)$ . As an example we show in Figure 6 the result for  $m = 0.04$ .

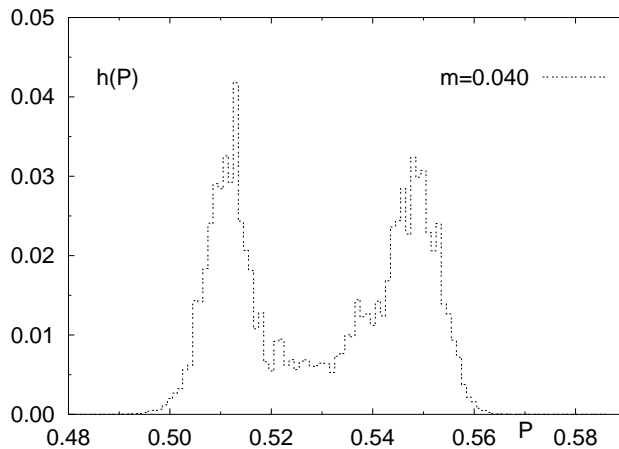


Figure 6: Distribution of the average plaquette values at  $\beta_c(m = 0.04)$  on a  $8^3 \times 4$  lattice obtained by reweighting results at nearby  $\beta$ -values.

The difference in the location of the two peaks in this distribution gives an estimate of the discontinuity in the plaquette expectation value. The results for different fermion masses are summarized in Table 5. A linear fit in the mass parameter yields the result at  $m = 0$ , which is given in the last column of Table 5. From this one

m	0.10	0.08	0.04	0.02	0.00
$\langle \Delta P \rangle$	0.0220 (9)	0.0227 (12)	0.0335 (29)	0.0308 (13)	0.0336 (16)

Table 5: Estimate of the discontinuity in plaquette expectation values at  $T_d$  for several values of the fermion mass. The last column gives the result of a linear extrapolation to the zero fermion mass limit.

obtains

$$\frac{\Delta\epsilon}{T^4} = 12.39 \pm 0.59 \quad (19)$$

as an estimate for the latent heat of the deconfinement transition.

In order to compare with corresponding results in the pure gauge sector we should relate the latent to the energy density of a free gas of gluons and adjoint fermions. Taking into account the known cut-off dependence of a free Bose and Fermi gas on lattices with a small temporal extent  $N_\tau = 4$  [20] we find  $\Delta\epsilon/\epsilon_{SB} = 0.306$  (15). This can directly be compared with the result in the pure gauge sector [19],  $\Delta\epsilon/\epsilon_{SB} = 0.31$  (3). We thus find that the latent heat per partonic degree of freedom is quite similar in the pure gauge theory and  $aQCD$  although in absolute units they differ quite a bit because 2-flavour  $aQCD$  has  $2 \cdot (N^2 - 1)(1 + 2 \cdot n_f) = 80$  degrees of freedom whereas the pure gauge theory only has  $2 \cdot (N^2 - 1) = 16$ .

Let us finally discuss the temperature dependence of the pressure,  $p/T^4$ . It generally is obtained from the plaquette expectation values shown in Figure 5 by subtracting the zero temperature expectation values for each value of the gauge coupling  $\beta$  and then integrating this difference as a function of  $\beta$  [17, 18]. Experience with similar calculations in the pure gauge sector shows that the zero temperature and finite temperature expectation values differ significantly only in the region where the finite temperature observable shows a rapid variation with  $\beta$ . The zero temperature expectation values only provide the subtraction of a smooth background. Without going through the complete calculation of the pressure we thus can deduce its structure already from the finite temperature data shown in Figure 5. The expectation values only show a rapid change at  $T_d$ . At the chiral transition point they are smooth. We thus find that also  $p/T^4$  will increase rapidly only at  $T_d$  and vary smoothly at  $T_c$ .

The chiral transition does not seem to leave a visible sign in bulk thermodynamic observables as it does not lead to a significant change in the number of light degrees of freedom at  $T_d$  as well as  $T_c$ . The number of Goldstone modes, which should be present up to  $T_c$ , is in the continuum limit about a factor eight smaller than the number of light adjoint fermions, which are liberated above  $T_d$ . However, our



calculation has been performed using the staggered fermion formulation, which only preserves a subgroup of the continuum  $SU(2n_f)$  flavour symmetry. The actual number of light modes thus is reduced and the total number of nine light Goldstone particles will only be recovered in the continuum limit. This may reduce their influence on the bulk thermodynamics in our present analysis. Clearly this aspect of the thermodynamics deserves further studies closer to the continuum limit.

## 4 Conclusions

We have shown that a  $SU(3)$  gauge theory with fermions in the adjoint representation leads to two distinct phase transitions at non-zero temperature. In the case of two Dirac fermions (simulated in the staggered fermion formulation) deconfinement occurs at a lower temperature than chiral symmetry restoration,  $T_c/T_d \approx 8$ . Unlike in  $QCD$  with fermions in the fundamental representation one thus has the possibility to examine the influence of both non-perturbative mechanisms on the thermodynamics separately. It will be interesting to analyze in the future in more detail the flavour dependence of  $T_c/T_d$ . In particular, it would be of interest to study both transitions in the *supersymmetric limit*, i.e. for  $n_f = 1/2$ .

We find that the deconfinement transition is first order for all values of the fermion mass and strongly influences the temperature dependence of bulk thermodynamic observables like the pressure as well as the screening of static charges in the fundamental and in the adjoint representation. The latent heat per degree of freedom is similar to that found in a pure  $SU(3)$  gauge theory and also the screening of static fermion charges, which sets in immediately above  $T_d$ , becomes stronger than in the pure gauge sector and thus reflects the increasing number of partons (bosons and fermions) participating in the screening of external charges.

The continuous chiral transition, on the other hand, does not seem to influence these observables significantly. We find, however, that chiral symmetry breaking in the deconfined region is significantly different from that in the confined region. Immediately above  $T_d$  the chiral condensate starts showing a much stronger fermion mass dependence than below  $T_d$ . The characteristic  $\sqrt{m}$ -dependence, which leads to a diverging fermion susceptibility as expected from the analysis of three dimensional  $\sigma$ -models, is clearly visible for  $T_d < T < T_c$ . As we use in our present analysis the staggered fermion formulation it is likely that only a small subset of the nine Goldstone modes present in the continuum are light in our lattice calculation. A more detailed analysis of the Goldstone modes closer to the continuum limit would certainly be of interest in the future.

**Acknowledgments** This work was partly supported by the TMR network *Finite Temperature Phase Transitions in Particle Physics*, EU contract no. ERBFMRX-CT97-0122. We thank J. Engels for helpful discussions on chiral singularities in the  $O(N)$  models and E. Laermann for numerous discussions as well as help in developing the programs used for our calculations.

## References

- [1] E.V. Shuryak, Phys. Lett. B107 (1981) 103.
- [2] R. Pisarski and F. Wilczek, Phys. Rev. D29 (1984) 339.
- [3] S. Gottlieb, W. Liu, D. Toussaint, R.L. Renken and R.L. Sugar, Phys. Rev. D35 (1987) 2531.
- [4] F. Karsch and E. Laermann, Phys. Rev. D50 (1994) 6954.
- [5] S. Aoki, M. Fukugita, S. Hashimoto, N. Ishizuka, Y. Iwasaki, K. Kanaya, Y. Kuramashi, H. Mino, M. Okawa, A. Ukawa and T. Yoshié, Phys. Rev. D57 (1998) 3910.
- [6] D.J. Wallace and R.K.P. Zia, Phys. Rev. B12 (1975) 5340.
- [7] J. Kogut, J. Polonyi, D.K. Sinclair and H. W. Wyld, Phys. Rev. Lett. 54 (1985) 1980.
- [8] J. B. Kogut, Phys. Lett. B187 (1987) 347.
- [9] M. E. Peskin, Nucl. Phys. B175 (1980) 197.
- [10] A. Smilga and J.J.M. Verbaarschot, Phys. Rev. D51 (1995) 829.
- [11] R. Kirchner, S. Luckmann, I. Montvay, K. Spanderen and J. Westphalen, *Evidence for discrete chiral symmetry breaking in  $N=1$  supersymmetric Yang-Mills theory*, DESY 98-165, hep-lat/9810062.
- [12] E. Witten, Adv. Theor. Math. Phys. 2 (1998) 505.
- [13] K. Bitar, A.D. Kennedy, R. Horsley, S. Meyer and P. Rossi, Nucl. Phys. B313 (1989) 348.
- [14] A.M. Ferrenberg and R.H. Swendsen, Phys. Rev. Lett. 63 (1989) 1195.
- [15] N.A. Campbell, I.H. Jorysz and C. Michael, Phys. Lett. 167B (1986) 91; for a recent discussion and further references see: J. Greensite, M. Faber and S. Olejnik, *Evidence for a center vortex origin of the adjoint string tension*, hep-lat/9807008.

- [16] C. DeTar, O. Kaczmarek, F. Karsch and E. Laermann, *String Breaking in Lattice Quantum Chromodynamics*, hep-lat/9808028, to appear in Phys. Rev. D.
- [17] G. Boyd, J. Engels, F. Karsch, E. Laermann, C. Legeland, M. Lütgemeier, B. Petersson, Nucl. Phys. B469 (1996) 419.
- [18] J. Engels, R. Joswig, F. Karsch, E. Laermann, M. Lütgemeier, B. Petersson, Phys. Lett. B396 (1997) 210.
- [19] Y. Iwasaki, K. Kanaya, T. Yoshie, T. Hoshino, T. Shirakawa Y. Oyanagi, S. Ichii and T. Kawai, Phys. Rev. D46 (1992) 4657.
- [20] J. Engels, F. Karsch and H. Satz, Nucl. Phys. B205 [FS5] (1982) 285.